JOURNAL OF AIRCRAFT
Vol. 37, No. 6, November–December 2000

Optimization for Fighter Aircraft Vertical-Plane Maneuvering Using Poststall Flight

Kazuhiro Horie* and Bruce A. Conway†
University of Illinois at Urbana–Champaign, Urbana, Illinois 61801

A time-optimal, vertical-plane, evasive-offensive maneuver using poststall flight is found for a fighter aircraft similar to an F-16. An evader aircraft initially followed by a pursuer aircraft transfers position using the vertical-plane maneuver, becoming the pursuer. The aircraft that was initially the pursuer is assumed to continue flight at constant velocity and constant altitude. A direct numerical method, collocation with nonlinear programming, proves well suited for solving this problem. The evader aircraft's optimal trajectory is found to be a cobra maneuver, one of the vertical poststall maneuvers. Allowing the evader to use thrust vectoring yields a small improvement in final time.

Nomenclature

C_D	=	drag coefficient
C_L	=	lift coefficient
D	=	drag force
$\boldsymbol{e}$	=	unit vector directed along the longitudinal axis of an evader
g	=	gravitational acceleration
h	=	altitude
J	=	cost function
L	=	lift force
m	=	mass
Nz	=	normal acceleration
$\boldsymbol{r}$	=	position vector of a pursuer relative to an evader
S	=	wing area
T	=	thrust
t	=	time
v	=	velocity
x	=	downrange position
α	=	angle of attack
γ	=	flight-path angle
ρ	=	air density
τ	=	thrust vectoring angle
τ_{LMT}	=	absolute value of limitation of thrust vectoring angle

Subscripts

e	=	value for initial evader
f	=	value at final time

Introduction

IN 1980, Herbst[1] suggested that poststall maneuverability should be one of the important design requirements for future fighter aircraft. He explained that poststall ability is "the ability of the aircraft to perform controlled tactical maneuvers beyond maximum lift angle of attack up to at least 70 degrees." The poststall maneuver gives an advantage of position in exchange for energy and minimizes the time for a turning maneuver. Many researchers have since studied optimal maneuvers using the poststall flight region. Well et al.[2] discussed a turning maneuver, a pointing maneuver, a slicing maneuver, and an evasive maneuver and concluded that use of the poststall region minimizes required time for these maneuvers. Bocvarov et al.[3] showed a time-optimal attitude reorientation using the poststall region. Uehara,[4] in a literature survey, discussed the role of poststall flight for enhancement of fighter maneuvering. He also pointed out the importance of using optimization theory in an analysis of enhanced maneuvering using poststall flight.

In 1989 the Su-27 fighter aircraft showed a new kind of poststall maneuver, the cobra maneuver, at the Paris air show.[5] This maneuver demonstrated a high angle of attack and low-speed flight after initial rapid pitching up in the vertical plane. Zagainov[6] published the Russian study related to the cobra maneuver done by the Su-27. He stated that the cobra maneuver has four distinguishing characteristics: the high angle of attack, the high initial pitch rate, the approximately 5-s maneuver time, and the large velocity loss. He concluded that the principal tactical advantages of the maneuver are that it allows weapon pointing irrespective of the direction of the aircraft motion and that it reduces the maneuver space, by which he meant that the pursuer flies by the evader due to a high aerodynamic deceleration. Murayama and Hull[7] regarded the cobra maneuver as "a maneuver which enables an evader to become a pursuer" and solved it numerically. They set a condition for termination of the cobra maneuver in which the evader transfers to a position 1000 ft behind the initial pursuer. Some of their solutions under additional terminal constraints were very similar to the cobra maneuver.

In this research, a minimum-time, vertical-plane, evasive–offensive maneuver, a maneuver in which the initial evader becomes the pursuer, is studied. The method of direct collocation with nonlinear programming (DCNLP), which has been successfully applied to many flight-path optimization problems, is used.[8–11] The aerodynamic model of Murayama and Hull[7] is used, and optimal trajectories with some of the same initial and terminal constraints are found, so that the results of using a different and more robust solution method (DCNLP) may be determined. In addition, the improvement in time of flight gained from having the capability of thrust vectoring is also found. The results are compared with the cobra maneuver, one of the poststall vertical maneuvers.

Problem Formulation

An air combat scenario is set by modifying a scenario used by Murayama and Hull.[7] The initial pursuer is in flight at constant velocity and constant altitude. The initial evader, an aircraft similar to an F-16, but which has the ability to fly in the poststall region, can maneuver in the vertical plane. At the final time, the evader transfers position and becomes able to attack the pursuer. An optimal trajectory for this maneuver is determined by how fast the evader can transfer position, that is, the cost function for this optimization problem is the time to completion of the evasive–offensive maneuver. The maneuver is illustrated in Fig. 1.

Received 12 July 1999; revision received 15 August 2000; accepted for publication 18 August 2000.

*Graduate Research Assistant, Department of Aeronautical and Astronautical Engineering.

†Professor, Department of Aeronautical and Astronautical Engineering; bconway@uiuc.edu. Associate Fellow AIAA.

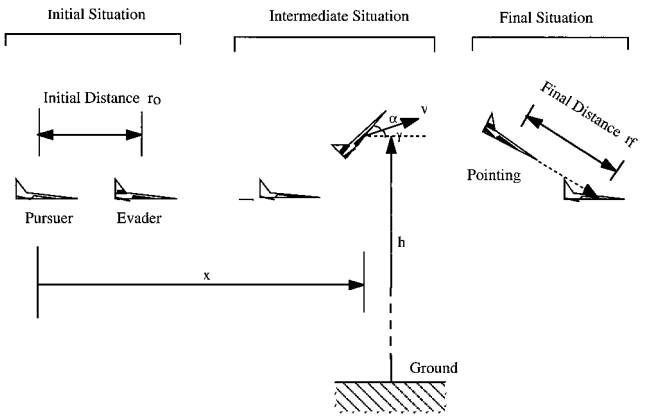

Fig. 1 Sequence of the evasive–offensive maneuver.

A set of equations of motion for the evader, a point mass model given by Vinh,[12] is modified to allow only motion in a vertical plane and to include a thrust vectoring angle τ:

$$\frac{dv}{dt} = \frac{1}{m}[T\cos(\alpha+\tau) - D] - g\sin\gamma \tag{1}$$

$$v\frac{d\gamma}{dt} = \frac{1}{m}[T\sin(\alpha+\tau) + L] - g\cos\gamma \tag{2}$$

$$\frac{dx}{dt} = v\cos\gamma \tag{3}$$

$$\frac{dh}{dt} = v\sin\gamma \tag{4}$$

where angle of attack α can take a value between 0 and 90 deg and τ ranges from $-\tau_{\mathrm{LMT}}$ to τ_{LMT}.

Because the maneuver time is very brief, the mass of the aircraft is assumed constant. The thrust is set to be equal to the weight of the aircraft. Aerodynamic data for the F-16-like maneuvering aircraft are essentially the same as used by Murayama and Hull.[7] A continuous approximation to their discrete tables of lift and drag coefficients is obtained using fourth-degree, piecewise polynomials found using least-square fitting under the constraint that they be continuous and at least twice differentiable everywhere.

The lift coefficient may be represented by

$$C_L = \begin{cases} 0.0174 + 4.3329\alpha - 1.3048\alpha^2 + 2.2442\alpha^3 \\ \quad - 5.8517\alpha^4 (0 \le \alpha \le \pi/6) \\ -1.3106 + 10.7892\alpha - 9.2317\alpha^2 - 1.1194\alpha^3 \\ \quad + 2.1793\alpha^4 (\pi/6 \le \alpha \le \pi/3) \\ 24.6577 - 71.0446\alpha + 83.1234\alpha^2 - 44.0862\alpha^3 \\ \quad + 8.6582\alpha^4 (\pi/3 \le \alpha \le \pi/2) \end{cases} \tag{5}$$

The drag coefficient may be represented by

$$C_D = \begin{cases} 0.0476 - 0.1462\alpha + 0.0491\alpha^2 + 12.8046\alpha^3 \\ \quad - 12.6985\alpha^4 (0 \le \alpha \le \pi/6) \\ 0.5395 - 5.7972\alpha + 21.6625\alpha^2 - 21.6213\alpha^3 \\ \quad + 7.0364\alpha^4 (\pi/6 \le \alpha \le \pi/3) \\ 16.6957 - 52.5918\alpha + 67.3227\alpha^2 - 37.086\alpha^3 \\ \quad + 7.4807\alpha^4 (\pi/3 \le \alpha \le \pi/2) \end{cases} \tag{6}$$

$$L = \tfrac{1}{2}\rho v^2 S C_L, \qquad D = \tfrac{1}{2}\rho v^2 S C_D \tag{7}$$

Atmospheric density, in the neighborhood of the nominal 10,000-ft altitude at which both airplanes are assumed to fly, is given as a function of altitude by[13]

$$\rho = \rho_s[1 - 0.00688(h/1000)]^{4.256} \tag{8}$$

where h is in feet and ρ_s is the sea-level atmospheric density.

The normal acceleration of the aircraft is restricted because of limits on structural strength and on the load a pilot can tolerate. This restriction is introduced as a path constraint:

$$Nz_{,\max} \ge Nz = (L\cos\alpha + D\sin\alpha + T\sin\tau)/mg \tag{9}$$

This research introduces a pointing constraint as a terminal constraint for the evasive–offensive maneuver. The pointing constraint requires that at the end of the maneuver the nose of the (original) evader aircraft points toward the (original) pursuer, with at least a given separation of the aircraft. This guarantees that the pilot of the evader aircraft would be able to see the opponent (i.e., that the pitch attitude of the airplane would not cause the opposing airplane to be obscured by the nose or forward fuselage of the airplane) and, of course, also point a weapon at the opponent. When $\boldsymbol{r}_f$ represents the position vector of the pursuer relative to the evader at the final time t_f, and with $\boldsymbol{e}$ being a unit vector directed along the longitudinal axis of the evader airplane, then

$$\boldsymbol{r}_f \cdot \boldsymbol{e} = \|\boldsymbol{r}_f\|\|\boldsymbol{e}\| = \|\boldsymbol{r}_f\| \tag{10}$$

Thus,

$$(v_e t_f - x_f)\cos(\gamma+\alpha) + (h_e - h_f)\sin(\gamma+\alpha) = \sqrt{(v_e t_f - x_f)^2 + (h_e - h_f)^2} \tag{11}$$

The separation constraint is

$$\|\boldsymbol{r}_f\| \ge r_{f,\min} \tag{12}$$

In addition to the pointing constraint, solutions are found with various additional terminal constraints. One is a constraint that the final velocity of the (original) evader, $v_e(t_f)$, be the same as that of the (original) pursuer. This prevents the evader aircraft, after it has exchanged position with the pursuing aircraft, from either rapidly overtaking or rapidly falling behind its opponent. Also, velocity loss should be avoided during air combat to maintain maneuverability for another engagement. Therefore, a constraint is introduced as a kinematic constraint:

$$v_e(t_f) = v_f \tag{13}$$

Another constraint is that the final flight-path angle of the evader be zero. As we assume that the (original) pursuer flies at a constant altitude, the evader cannot continue following the pursuer if the flight-path angle is not zero. Therefore, a following constraint is introduced as

$$\gamma_f = 0 \tag{14}$$

Murayama and Hull[7] used a final horizontal distance between the evader and pursuer as a terminal constraint. In this paper, their primary constraint is called a horizontal distance constraint. It is expressed as

$$r_{hc} = v_e t_f - x_f \tag{15}$$

where r_{hc} is the desired horizontal separation at the final time. In some cases, they also applied a constraint we term the altitude constraint

$$h_f = h_e \tag{16}$$

requiring the evader to return to its original altitude (which is the same as the altitude of the original pursuer). In this work, the horizontal distance constraint and/or the altitude constraint are applied so that current results may be compared with the corresponding Murayama and Hull[7] results.

Aircraft dimensions, physical constants, and initial conditions necessary for the numerical solutions are shown in Table 1. The numerical solution is facilitated by converting the customary length, time, and mass units into nondimensional units also shown in Table 1.

Table 1 Data and initial condition for numerical analysis

Quantities	Dimensional value	Nondimensional value
Mass of aircraft m	637.16 slug	1.0
Thrust T	20,500 slug · ft/s^2	0.80435
Air density at sea level ρ_s	1.7556×10^{-3} slug/ft^3	1.76340×10^5
Gravitational acceleration g	32.174 ft/s^2	0.80435
Wing area S	300.0 ft^2	1.875×10^{-5}
Max. normal acceleration Nz	9.0 g	9.0
Velocity of initial pursuer v_e	400.0 ft/s	1.0
Altitude of initial pursuer h_e	10,000 ft	2.5
Initial distance between evader and pursuer r_0	1,000 ft	0.25
Min. final distance between evader and pursuer $r_{f,\min}$	1,000 ft	0.25
Initial velocity of evader v_0	400.0 ft/s	1.0
Initial flight-path angle of evader γ_0	0.0 rad	0.0
Initial horizontal position of evader x_0	1,000 ft	0.25
Initial altitude of evader h_0	10,000 ft	2.5

Flight-Path Optimization

The optimal control problem may be expressed as

$$\min_{u(t)} J[\boldsymbol{x}(t), \boldsymbol{u}(t), t_f] \tag{17}$$

subject to

$$\dot{\boldsymbol{x}}(t) = \boldsymbol{f}[\boldsymbol{x}(t), \boldsymbol{u}(t)] \tag{18}$$

$$\boldsymbol{g}[\boldsymbol{x}(t), \boldsymbol{u}(t)] \leq \boldsymbol{0} \tag{19}$$

where $\boldsymbol{x}(t)$ is the vector of state variables and $\boldsymbol{u}(t)$ is the vector of control variables. Equation (18) are the equations of motion and Eq. (19) represents a vector of inequality constraints consisting of the bound of state and control variables, path constraints, terminal constraint, and specific initial and terminal conditions.

A highly accurate DCNLP method due to Herman and Conway[10] is used to convert the optimal control problem (17–19) into a nonlinear programming problem. In the DCNLP method, the total time history is divided into segments (usually of equal duration). The boundaries of each time segment are termed nodes; it is at these points that discrete values of the states and controls are defined (as parameters). In this research, the state time history between nodes is assumed to be given by a fifth-degree polynomial (in time). Herman and Conway[10] showed that this DCNLP is equivalent to integration using a fifth-degree Gauss–Lobatto quadrature rule. The high-degree polynomial approximation characterizes this method as much more accurate than the standard DCNLP.

The maneuver period is divided into 20 equal segments. The six quantities necessary to uniquely specify a fifth-degree polynomial are available as the values of the states and the value of the slope of the polynomial at the left, center, and right sides of the segment. The state and control variables are discretized to specify a fifth-degree polynomial for each segment. The set of parameters to be optimized, $\boldsymbol{P}$, consists of discretized state variables, discretized control variables, and total time t_f, i.e.,

$$\begin{aligned}\boldsymbol{P} = \{&\boldsymbol{x}(t_0), \boldsymbol{x}(t_{c,0}), \boldsymbol{x}(t_1), \boldsymbol{x}(t_{c,1}), \boldsymbol{x}(t_2), \ldots, \boldsymbol{x}(t_{c,n-1}), \boldsymbol{x}(t_n), \boldsymbol{u}(t_0),\\ &\boldsymbol{u}(t_{1,0}), \boldsymbol{u}(t_{c,0}), \boldsymbol{u}(t_{2,0}), \boldsymbol{u}(t_1), \boldsymbol{u}(t_{1,1}), \boldsymbol{u}(t_{c,1}), \boldsymbol{u}(t_{2,1}),\\ &\boldsymbol{u}(t_2), \ldots, \boldsymbol{u}(t_{2,n-1}), \boldsymbol{u}(t_n), t_f\}\end{aligned} \tag{20}$$

where t_i is the time at the ith node; $t_{c,i}$ is the time at the center of the $(i+1)$th segment; $t_{1,i}$ and $t_{2,i}$ are times within the $(i+1)$th segment, to the left and right of the center of the segment, respectively; and t_n and t_f are both the final time.[10]

The optimal solution is found in variable space $\boldsymbol{P}$ under constraints. Because all constraints are described in algebraic form, Eqs. (17–19) can be rewritten as the nonlinear programming problem:

$$\min_{\boldsymbol{P}} J(\boldsymbol{P}) \tag{21}$$

subject to

$$\boldsymbol{h}(\boldsymbol{P}) \leq \boldsymbol{0} \tag{22}$$

Equation (22) consists of a set of nonlinear constraints that, if satisfied, include or are equivalent to integration of the system equations across the ith segment using the fifth-degree Gauss–Lobatto integration rule,[10] the bounding of state and control variables, path constraints, terminal constraints, and specific initial and terminal conditions. A set of parameters satisfying Eqs. (21) and (22) is a solution of the optimal control problem.

NZSOL[14] is used to solve the nonlinear programming problem just introduced. A Hewlett–Packard C-160 computer is used to implement the numerical optimization.

Results and Discussion

Optimal flight paths are found for three different combinations of terminal constraints; all of the solutions include the constraint on vertical acceleration (9) and all assume that the aircraft that is initially the pursuer maintains constant level flight. Both a feasibility parameter and an optimality tolerance parameter in NZSOL are set at 10^{-8}. The use of DCNLP gives convergent solutions without special treatments for all cases.

The result of applying the pointing constraint given by Eqs. (11) and (12) is shown in Figs. 2 and 3. Figures 2 and 3 show that the maneuver may be divided into three phases. In the first phase, the evader has an angle of attack between 40–80 deg and establishes a climb. In the second phase, the evader aircraft has a 90-deg angle of attack and experiences dramatic aerodynamic deceleration. In the third phase the aircraft establishes an angle of attack of 0 deg, begins to descend, and finally points its longitudinal axis toward its

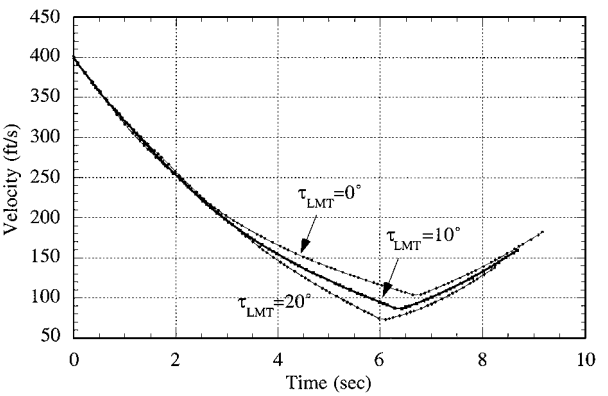

Fig. 2 Velocity history for case with pointing constraint alone.

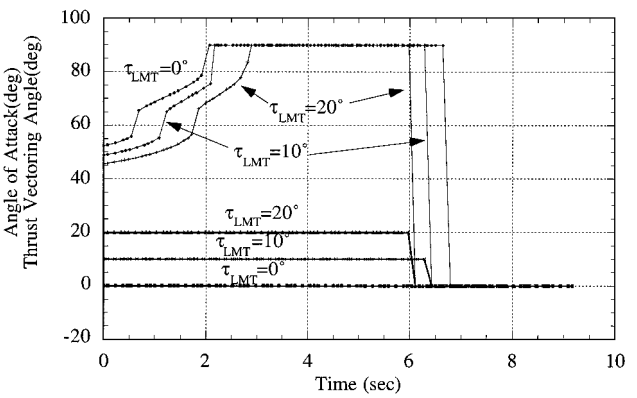

Fig. 3 Control variables history for case with pointing constraint alone.

target, the (original) pursuer aircraft. This result includes two of the characteristics of the cobra maneuver, the high angle of attack and the large velocity loss. The maneuver time of about 2 s is essentially the same as the cobra maneuver time described by Zagainov.[6] Physically, the first two phases are explained as phases for rapid deceleration so that the evader will be passed by the pursuer. By establishing a positive flight-path angle by the nose-up motion, the evader decelerates using drag but also gravity. After establishing sufficient flight-path angle, the evader maximizes drag force with a vertical attitude. After enough deceleration, the evader takes a zero angle of attack so that it can satisfy the pointing terminal constraint. The deceleration, from an initial speed of 400 ft/s, is very rapid, and although some speed is recovered in the third phase, the airplane ends with a speed less than 200 ft/s, as seen in Fig. 2. When the use of thrust vectoring is permitted, the deceleration during the first two phases is supplemented by choosing a full positive thrust vectoring angle, as seen in Fig. 3. The final time for the maneuver using thrust vectoring is 8.24 s, in the case of a thrust vectoring authority of 20 deg, whereas that without thrust vectoring is 9.16 s. The maximum normal acceleration is around 5.1 g and does not violate the path constraint. Figure 4 shows the trajectories of the two aircraft for a case using thrust vectoring capability, as well as how the evader becomes the pursuer.

Adding the kinematic constraint [Eq. (13)] to the pointing constraint [Eqs. (11) and (12)] yields results shown in Figs. 5 and 6. The requirement of Eq. (13) that the final speed of the (original) evader match the constant speed of the (original) pursuer, 400 ft/s, yields a substantially different flight path from that of the earlier case, that is, the evader descends instead of climbing. Figure 6 shows that there are still three different phases to the maneuver, but they are different from those of the earlier case having only the pointing constraint, which was shown in Fig. 3. The first phase is the vertical phase for taking a maximum drag force. The airplane stands on its tail immediately, rather than gradually as in Fig. 3. Next, the evader takes a zero angle of attack to descend and accelerate to satisfy the kinematic condition. During the final phase of the maneuver, the

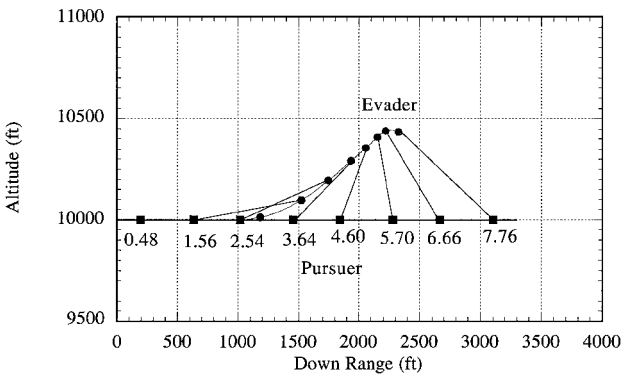

Fig. 4 Trajectories of the evader and pursuer for case with pointing constraint alone (maximum thrust vectoring angle = 20 deg).

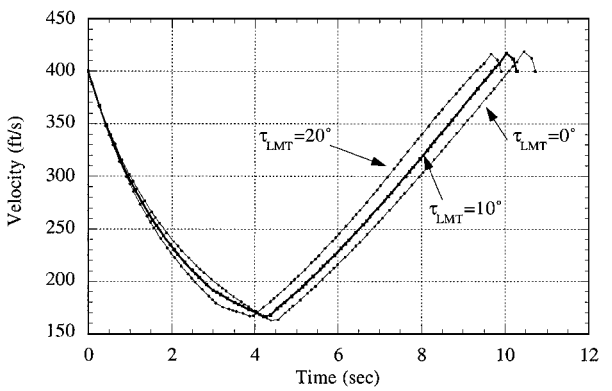

Fig. 5 Velocity history for case with pointing and kinematic constraints.

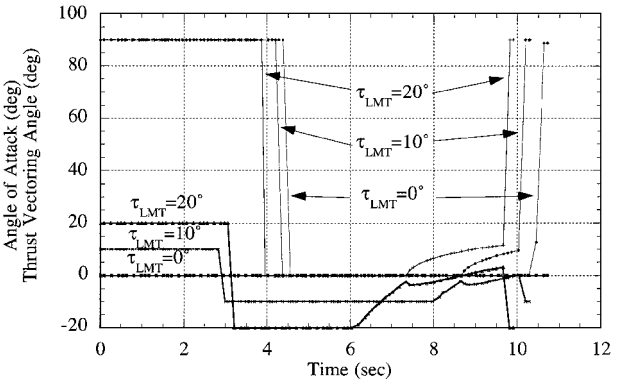

Fig. 6 Control variables history for case with pointing and kinematic constraints.

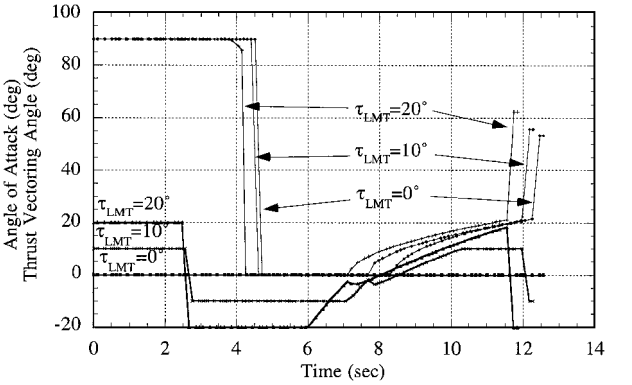

Fig. 7 Control variables history for case with pointing, kinematic, and following constraints.

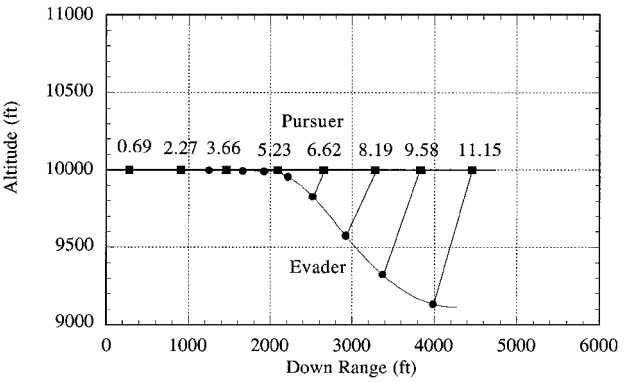

Fig. 8 Trajectories of the evader and pursuer for case with pointing, kinematic, and following constraints (maximum thrust vectoring angle = 20 deg).

evader increases the angle of attack, aligns its velocity to the constraint value, and points toward the pursuer, which requires a very high angle of attack because the pursuer is close and above.

Adding the following constraint Eq. (14) to the pointing and kinematic constraints does not dramatically change the angle-of-attack history or the trajectory, though it does significantly increase the maneuver time. Figure 7, showing angle of attack for this case, is very similar to the corresponding result shown in Fig. 6, except that at the end the requirement of horizontal flight reduces the final angle of attack. The trajectories of the evader and pursuer are shown in Fig. 8.

Thrust vectoring ability is used to enhance not only the combat maneuverability, but also aircraft stability in the post-stall region. In addition, an increase in the thrust vectoring authority always reduces the time required for the maneuver, as shown in Fig. 9, that is, using the thrust vectoring ability decreases the duration that the evader is followed by the pursuer. In combat that would, of course, be beneficial to the evader.

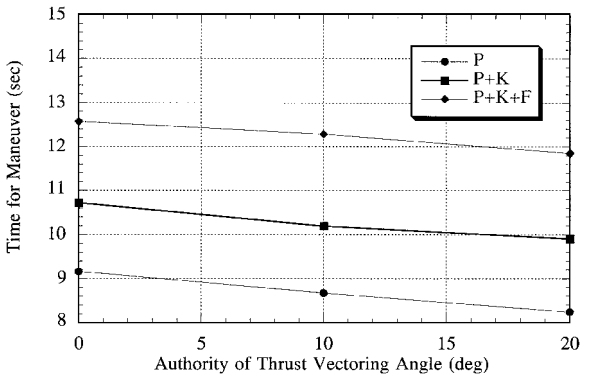

Fig. 9 Sensitivity of maneuver time to thrust vectoring capability: P, case with pointing constraint; P+K, case with pointing and kinematic constraints; and P+K+F, case with pointing, kinematic, and following constraints.

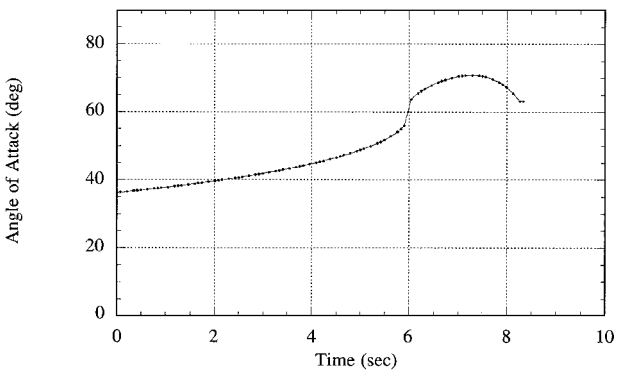

Fig. 10 Control variables history in case I.

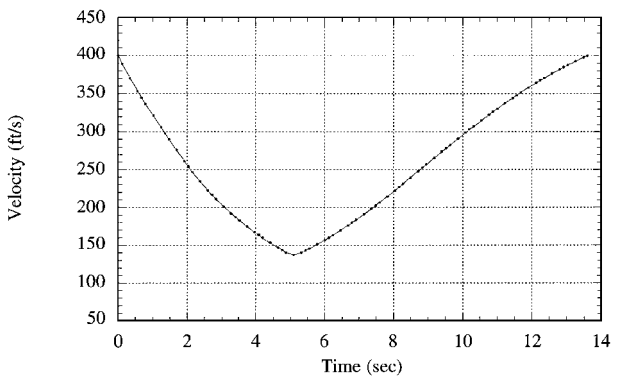

Fig. 11 Velocity history in case IV.

Because the aircraft, initial conditions, and terminal conditions were in some instances made the same as those Murayama and Hull[7] used in their research a direct comparison of results is possible. (Note that the names case I, case II, etc., are those used in Ref. 7.)

For case I, employing the horizontal distance constraint (15), the control time history in this research (shown in Fig. 10) is qualitatively different from that of Murayama and Hull (cf. Fig. 4 in Ref. 7). Despite this, the final time for the maneuver found in this research, 8.33 s, is essentially equal to their result.

For case II, employing the horizontal distance and following constraints (15) and (14), the results for the control and state variable histories are qualitatively the same. However, there is a small difference in the final time of the maneuver, 8.97 s in this research vs 9.3 s in the Murayama and Hull research.[7]

For case IV, employing the horizontal distance, kinematic, following, and altitude constraints (15), (14), (13) and (16), the velocity history (Fig. 11) is different from that found by Murayama and Hull (cf. Fig. 7 in Ref. 7) as is the control time history. The final time for the maneuver in this research, 13.60 s, is substantially different from (and improved from) that in their research, which was 16.3 s (Ref. 7).

These differences may be explained by the solution method in this research using very accurate, high-order, implicit integration. The Murayama and Hull convergence tolerance[7] is 10^{-4}, whereas in this research 10^{-8} is used. In addition, this research uses many more discrete control variables, 81 vs 11 for Murayama and Hull,[7] over the maneuver time span, thus capturing better the control time history.

Conclusions

With a model aircraft similar to an F-16, but with the capability of poststall flight, the minimum-time, vertical-plane, evasive–offensive maneuver has been found. The evader aircraft quickly exchanges position so that it becomes the pursuer. The optimal trajectories and the angle-of-attack history of the airplane qualitatively resemble those described as the cobra maneuver. Thrust vectoring authority reduces the flight time for the evasive–offensive maneuver, decreasing the exposure of the evader to attack by the pursuer.

Perhaps the most significant result is that the DCNLP method has solved this problem successfully and robustly for a variety of terminal constraints. We thus recommend it as an appropriate method for trajectory optimization for maneuverable aircraft.

For future study, the equations of motion should be expanded from a point-mass model to a rigid-body model. The principal effect of this improvement would be to moderate the initial rapid nose-up motion, which is nearly instantaneous in this work, and, thus, generate a more accurate flight-path. A more ambitious improvement would be to introduce a differential game formulation to this problem that can deal with the pursuer as a realistic, maneuvering aircraft and find optimal trajectories for both evader and pursuer.

Acknowledgment

This study was partially funded by the Boeing Information, Space, and Defense Systems Company under Contract JR-7231.

References

[1]Herbst, W. B., "Future Fighter Technologies," *Journal of Aircraft*, Vol. 17, No. 8, 1980, pp. 561–566.

[2]Well, K. H., Faber, B., and Berger, E., "Optimization of Tactical Aircraft Maneuvers Utilizing High Angle of Attack," *Journal of Guidance, Control, and Dynamics*, Vol. 5, No. 2, 1982, pp. 131–137.

[3]Bocvarov, S., Lutze, F. H., and Cliff, E. M., "Time-Optimal Reorientation Maneuvers for a Combat Aircraft," *Journal of Guidance, Control, and Dynamics*, Vol. 16, No. 2, 1993, pp. 232–240.

[4]Uehara, S., "A Trend of the Pursuit–Evasion Problem of High Speed Aircraft: Maneuverability Plus Agility," *Journal of the Japan Society of Aeronautical and Space Sciences*, Vol. 46, No. 5, 1998, pp. 261–270 (in Japanese).

[5]"Agile Sukhoi Su-27 Leads Strong Soviet Presentation," *Aviation Week and Space Technology*, Vol. 130, No. 25, 1989, pp. 28–30.

[6]Zagainov, G., "High Maneuverability, Theory and Practice," AIAA Paper 93-4737, 1993.

[7]Murayama, K., and Hull, D. G., "Cobra Maneuver as Minimum Time Problem," *Proceedings of the AIAA Atmospheric Flight Mechanics Conference*, AIAA, Reston, VA, 1997, pp. 339–344.

[8]Hargraves, C. R., and Paris, S. W., "Direct Trajectory Optimization Using Nonlinear Programming and Collocation," *Journal of Guidance, Control, and Dynamics*, Vol. 10, No. 4, 1987, pp. 338–342.

[9]Enright, P. J., and Conway, B. A., "Optimal Finite Thrust Spacecraft Trajectories Using Collocation and Nonlinear Programming," *Journal of Guidance, Control, and Dynamics*, Vol. 14, No. 5, 1991, pp. 981–985.

[10]Herman, A. L., and Conway, B. A., "Direct Optimization Using Collocation Based on High-Order Gauss–Lobatto Quadrature Rules, *Journal of Guidance, Control, and Dynamics*, Vol. 19, No. 3, 1996, pp. 592–599.

[11]Ryan, G. W., III, and Downing, D. R., "Evaluation of Several Agility Metrics for Fighter Aircraft Using Optimal Trajectory Analysis," *Journal of Aircraft*, Vol. 32, No. 4, 1995, pp. 732–738.

[12]Vinh, N. X., *Optimal Trajectories in Atmospheric Flight*, Elsevier, Amsterdam, 1981, pp. 50–62.

[13]McCormick, B. W., *Aerodynamics, Aeronautics and Flight Mechanics*, Wiley, New York, 1994, p. 24.

[14]Gill, P. E., Saunders, M. A., and Murray, W., *User's Guide for NZOPT 1.0: A Fortran Package For Nonlinear Programming*, McDonnell Douglas Aerospace, Huntington Beach, CA, 1993.